RSC Advances

Differential dynamic behavior of Interaction of some common derivatives of Acridine class molecules with CT DNA: deciphering the modes in nanosecond and femtosecond time domain

Journal:	*RSC Advances*
Manuscript ID:	RA-ART-07-2015-013035.R2
Article Type:	Paper
Date Submitted by the Author:	24-Aug-2015
Complete List of Authors:	Basu, Samita; Saha Institute of Nuclear Physics, Chemical Sciences Sengupta, Chaitrali; saha institute of nuclear physics, chemical sciences division

A spectroscopic study to decipher the mode of Interaction of some common Acridine derivatives with CT DNA within nanosecond and femtosecond time domain.

Chaitrali Sengupta and Samita Basu*

Chemical Sciences Division,

Saha Institute of Nuclear Physics, 1/AF, Bidhannagar,

Kolkata 700 064, India

***Corresponding Author:**

E-mail address: samita.basu@saha.ac.in.

Telephone: +91-33-2337-5345, Fax: +91-33-2337-4637

Abstract: Acridine and other derivatives of this class are very familiar as DNA intercalators. We, in our present contribution, have taken an attempt to decipher the exact mode of interaction of acridine and some of its derivatives, e.g. acridine yellow, proflavine and acridine orange, with calf thymus DNA (CT DNA). Primarily, all these molecules undergo intercalation inside DNA. The simple acridine molecule undergoes complete intercalation. However, the derivatives with flanking substituents have to traverse some steps before intercalation which favor subsequent photoinduced electron transfer (PET) with DNA bases. The steady state and time resolved spectroscopic studies within nanoseconds to subpicoseconds time regime have revealed the exact timescale of the stepwise intercalation and PET. It has been seen that bound water molecules in the near vicinity of DNA molecule play a pivotal role in determining the timescales. The structure of bound water and its exchange with surrounding bulk water often take an important role in many processes of life involving DNA. Moreover, our investigation clearly depicts how the increased number of electron donating side groups present in the derivatives becomes the deciding factor, both electronically and sterically, in controlling the differential behavior of the individual molecules towards PET in CT DNA environment.

Introduction:

Deoxyribonucleic acid (DNA) is the basic unit of most living organism on earth that actually contains and bears the genetic instructions and determines the development of other components like protein, RNA and cells. The organized double helical structure of DNA potentiates many fascinating physical phenomena to be occurred within it, among which long range charge transfer through consecutive base stacks is the most cultivated one. Eley and Spivey are the pioneers in conceiving the idea about the regularly stacked B-form DNA which might serve as a pathway for charge transfer (CT) processes.[1] Since then the question has been raised by the scientists whether the double helix structure of DNA, a macromolecular assembly in solution with π-stacked base pairs, resembles the conductive characteristics with π-stacked solids. During 1990s' Barton and co-workers reported the occurrence of DNA- CT in several donor-acceptor systems, where the characteristics of DNA charge transport had been exploited using non covalently bound metal complexes as DNA intercalators to initiate charge injection.[2] Later many research groups investigated over the recognition of small intercalators with DNA and the role that they play in long range DNA-CT as this phenomenon is an important mechanism of photoinduced DNA damage leading to mutation, apoptosis and cancer.[3-7] The CT is an operative mechanism which senses DNA damage as well as initiates its repair.[8]There are two types of DNA-mediated CT processes, oxidative hole transfer and reductive electron transfer, as depicted

in literature. After photoexcitation whether the intercalator would take part in reduction (i.e. donation of electron) or oxidation (generation of hole) that depends on the deference in reduction potential between the intercalator and the bases present at intercalation site.

Several research groups are interested about DNA-CT. Some of the groups investigated the phenomenon through photoinduced charge injection as well as dynamical fluorescence and excited state absorption studies where the rest tried to probe DNA CT through electrochemical methods taking advantage of development of metals, carbon based electrodes and semiconductors which react with nucleic acids to lesser extent than previously used mercury electrodes.[9] In most of the cases, photochemical investigation of DNA-CT was initiated by absorption of photon that provides sufficient amount of energy to make CT an exergonic process.The extent of DNA- CT depends on several factors. Each type of DNA necessarily does not mediate long range CT. Proper structure and conformational dynamics control the necessary coupling between base pairs to occur CT over the long distance. At experimental condition, i.e. at nonzero temperature it is obvious that there would be conformational fluctuations, however only those fluctuations which are large could perturb the rate constants of the CT processes. Moreover the conformational gating helps to increase the extent of CT rather than to decrease it.[10] Photoexcited$[Rh(phi)2(bpy')]^{3+}$ and ^{CP}G were tethered to measure the temperature dependence of CT in DNA.[11] For all the bridges, the efficiency of CT increases with temperature and the temperature dependence is greater with increasing bridge length.

An alternative mechanism of CT through DNA was also postulated by Brillouin *et al*.[12] The charge conduction of DNA can occur through the phosphate backbone. In this phosphate conduction model, the phosphate molecules on the edge of DNA are directly ionized, and the

holes hop rapidly through the isoenergetic phosphates. However this would happen only when the coupling among the phosphates is substantial.[13] Some calculations show the preference of oxidative holegeneration at phosphates over DNA bases. However later, theoretical calculations pointed out the mistake of neglecting the presence of water and counter ions which shield the negative charges of the phosphate groups.[14] It was already shown both experimentally and theoretically that photoionization occurs at bases, but not at the phosphates.[15]

The chemistry and photophysics of the photoexcited acridine (Acr*) containing systems, which mediate CT over only a few base pairs, were extensively studied by some research groups.[16, 17] Feilitzsch *et al* reported 9-amino-6-chloro-2-methoxyacridine as an intercalated acridine derivative in DNA that helps to investigate the effect of site of intercalation and the dependence of base stacking sequence on the rate of CT by photochemical and NMR spectroscopic methods.[16] They showed that a change in a single base matching induces a difference in rate of CT by a factor of two which can be clearly explained by classical Marcus theory on the basis of free energy difference between guanine and deazaguanine. Hess et al. reported the excited state dynamics of the same located at a specific base site of DNA to account for their local solvation within DNA interior.[18] Kuruvilla *et al.* reported the effect of substitution at the ninth position of the acridinium ring by 2-methylphenyl and 2,4-dimethylphenyl substituents regarding DNA binding and specific interactions with sequence specific DNA oligonucleotides.[19]

In our present contribution, we have taken an attempt to investigate the differential behavior of some common acridine derivatives with calf thymus DNA to decipher the factors playing to determine the feasibility of electron transfer (ET) through base stacks. Steady-state absorption

and fluorescence, time-resolved fluorescence and circular dichroism techniques have been employed to investigate the electronic and steric control over DNA binding and ET.

Figure:-1

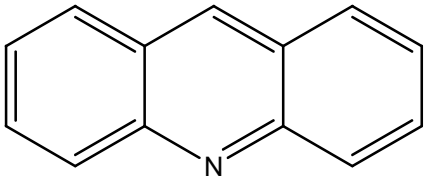

Acridine

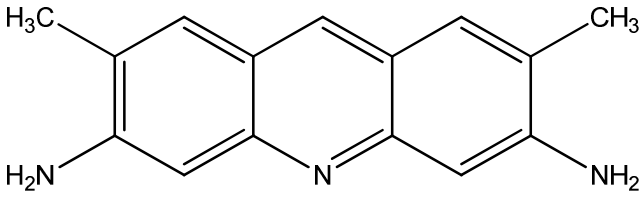

Acridine yellow

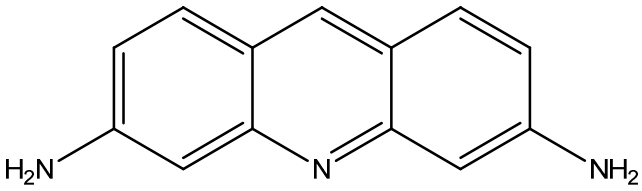

Proflavine

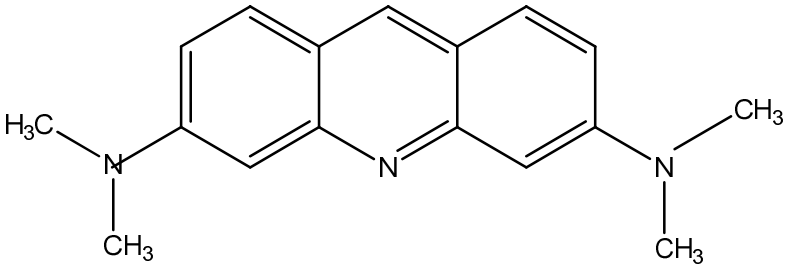

Acridine orange

Materials and Methods

Reagents and Sample preparation: All the chemicals used here are purchased from Sigma-Aldrich and used without further purification. The structures of Acridine, Acridine Yellow , Proflavine and Acridine Orange are given in figure 1. Water is triply distilled before use. Solutions are prepared by dissolving CT DNA in Tris-HCl buffer (pH~7.2) by volumetric method. Tris-HCl buffer was prepared dissolving Tris and NaCl in required amount in water amd adjusting pH to 7.2 by adding Conc. HCl. All the solutions of dyes and CT DNA are prepared in Tris-HCl buffer (pH~7.2). According to Porsch, plausible calf-thymus DNA molecular weight distribution can be obtained by size-exclusion chromatography with dual low-angle light scattering/ refractometric detection at sufficiently low flow rate. The distribution extends over three decades of molecular weight and is characterized by weight average molecular weight ($M_{w)}$ = 8418000 and polydispersity index (M_w /M_n)= 5.2.[35] CT DNA is taken in an arbitrary amount and dissolved in minimum volume of buffer. The concentration of DNA in the solution was determined spectrophotometrically measuring absorbance (A) obtained directly from the spectral data) and following Lambert Beer Law: A = ϵ.C.l, C=DNA concentration in cuvette, l = path length of the quartz cuvette. using the molar extinction coefficient (ϵ) for CT DNA = 6600 cm^{-1} M^{-1}/base at 260 nm. The concentration of all the dye molecules are kept at 0.01 mM in Tris-HCl buffer (pH~7.2) and the DNA concentration is varied as per requirement during experiment.

Absorption and Fluorescent measurements: Steady state absorption and fluorescence spectra of all these dyes were recorded by using JASCO V-650 absorption spectrophotometer and Spex Fluoromax-3 Spectro-fluorimeter respectively using a 1.0 cm path length quartz cuvette. While performing the absorption experiment, a reference cuvette has been used with same volume of

buffer and each time required amount of DNA solution has been added to the reference cuvette for baseline correction. For a given sample, the wavelength at which absorbance is maximum (λ_{max}) is used as excitation wavelength for corresponding emission scan. Time-resolved emission spectra of all these dyes in absence and presence of CT DNA were performed using a picosecond pulsed diode laser based TCSPC fluorescence spectrometer with λ_{ex} ~ 377 nm (for acridine) and λ_{ex} ~ 470 nm (for acridine yellow, proflavine, acridine Orange) and MCP-PMT as a detector. The emission from the samples is collected at a right angle to the direction of the excitation beam maintaining magic angle polarization (54.7°) with a bandpass of 2 nm. The full width at half maximum (FWHM) of the instrument response function is 270 ps and the resolution is 28 ps per channel. The data are fitted to exponential functions after deconvolution of the instrument response function by an iterative reconvolution technique using data analysis software (IBH DAS 6.2) in which reduced χ^2 and weighted residuals serve as parameters for goodness of fit. All the steady-state and time-resolved measurements are performed at room temperature (298K).

For time-resolved fluorescence anisotropy decay measurements, the polarized fluorescence decays for the parallel [I_{VV}] and perpendicular [I_{VH}] emission polarizations with respect to the vertical excitation polarization are first collected at the emission maxima of the drug. The anisotropy decay function r(t) is constructed from these I_{VV} and I_{VH} decays using the standard procedure.[33]

Femtosecond fluorescence up-conversion measurements: The fluorescence transients are measured by a femtosecond fluorescence up-conversion setup (FOG-100, CDP Corporation). The sample is excited at 400 nm with full excitation slit width using the second harmonic of a mode-locked Ti-sapphire laser (Mai Tai, Spectra Physics), pumped by a 5 WMillennia (Spectra

Physics). To generate second harmonic we used a nonlinear crystal (1 mm BBO, θ = 38°, φ = 90°). The fluorescence emitted from the sample was obtained under the magic angle configuration and is up-converted in another nonlinear crystal (0.5 mm BBO, θ = 38°, φ = 90°) by using the fundamental beam as a gate pulse. The up-converted light is dispersed in a monochromator and detected by photon counting electronics. The femtosecond fluorescence decays were deconvoluted using a Gaussian shape for the instrument response function having a FWHM of ~206 fs (obtained through water Raman scattering) using commercial software (IGOR Pro, Wave Metrics, USA). The decay traces are recorded at different wavelengths which will be reported at their respective places in the paper. They were also fitted and analyzed using IGOR Pro software to obtain fluorescence decay times.

Circular dichroism spectroscopy: CD spectra of CT DNA are monitored in a Chirascan CD Spectrometer from Applied Photophysics. Acquisition duration is fixed at 2 seconds and the wavelength range (220 – 340 nm) was scanned at 0.5 nm intervals keeping a bandwidth of 1 nm. Each spectrum is an average of 3 accumulations.

The software ORIGINPRO 7.5 and ORIGINPRO 8.0 is used for curve drawing for all experiments except Femtosecond resolved fluorescence upconversion experiments.

Viscometric study: An ubbelohde viscometer is used for viscosity measurement. This type of viscometer is used to obtain a lower velocity gradient. Ubbelohde viscometer has been frequently used to determine the molecular weights of proteins which are also expected to be Non-Newtonian fluids (velocity gradient ranges covered were within 0.6 – 120,000 sec^{-1}).[38] In case of our DNA solution the range of velocity gradient was within the covered range mentioned above. The relative viscosity (η) of the DNA-dye system has been determined using the following

equation $\eta = t/t_0$, where t_0 is the flow time for tris buffer alone and t is the flow time of either only CT-DNA solution or DNA solution in presence of different concentrations of the complexes. The mean of three replicated measurements was taken during this experiment.

Results and Discussion

Absorption Studies: All the acridine derivatives namely, acridine, acridine yellow, proflavine and acridine orange show slightly different absorption and fluorescence spectra and respond differently in presence of DNA. Figure 2 (a), (b), (c) and (d) are the representative spectra of acridine, acridine yellow, proflavin and acridine orange respectively with increasing concentration of CT DNA

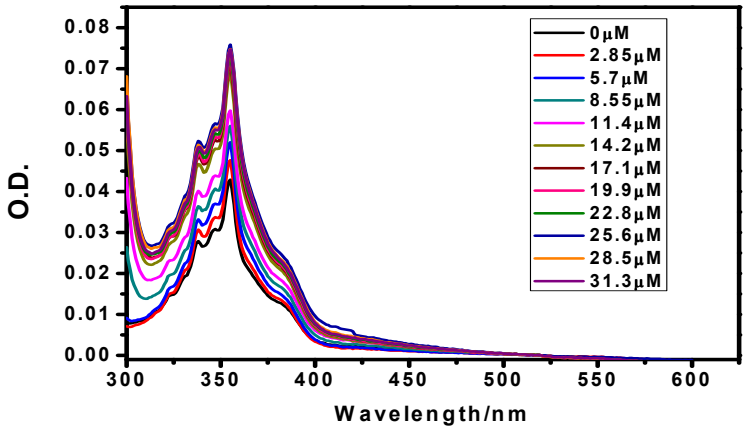

Figure 2(a): Absorption spectra of acridine (0.01mM) in absence and presence of varying concentration of CT DNA.

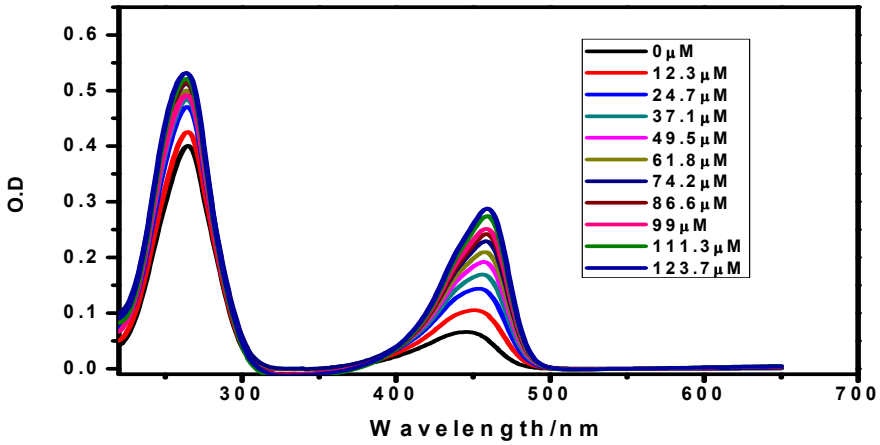

Figure 2(b): Absorption spectra of acridine yellow (0.01mM) in absence and presence of varying concentration of CT DNA.

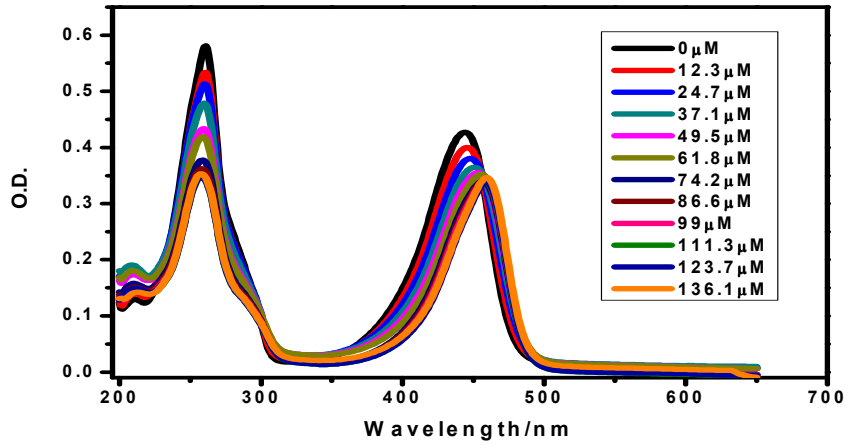

Figure 2(c): Absorption spectra of proflavine (0.01mM) in absence and presence of varying concentration of CT DNA.

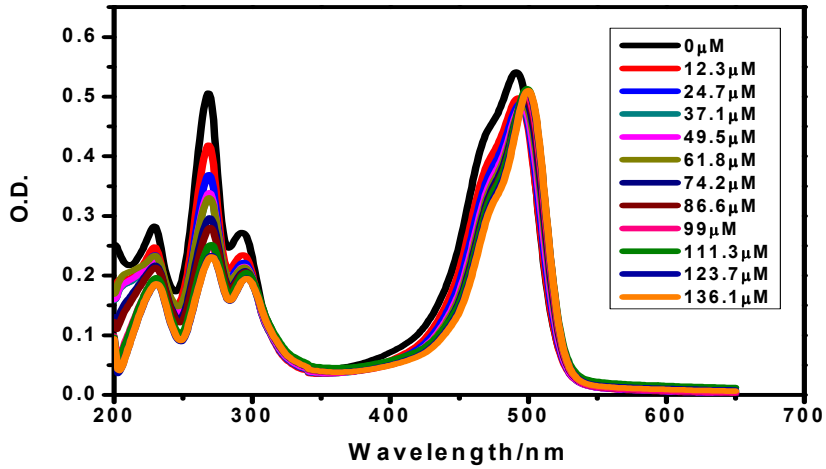

Figure 2(d): Absorption spectra of acridine orange (0.01mM) in absence and presence of varying concentration of CT DNA.

Acridine and all the other derivatives are well known as DNA intercalator due to their planar structure. Still, their responses towards DNA, which are quite different from each other, intrigue us to search the specific binding modes of the dyes with DNA individually. Simple acridine molecule undergoes only an increment in absorbance value without any sort of shift in absorption maximum, while proflavine and acridine orange show hypochromism along with a red shift of absorption maximum (λ_{max}) at 445 nm and 492 nm respectively. With a sharp contrast to all of them, acridine yellow leaves a signature of hyperchromism accompanying a red shift with increasing concentration of DNA. In case of acridine, the increase in absorbance indicates an interaction between acridine and DNA strand, but the unaltered absorption maximum discards any possibility of its further stabilization upon intercalation. Here, the absorption spectra indicate that the fully intercalated acridine absorbs in the same region as free acridine in buffer. On the other hand proflavine and acridine orange interact in a very similar

way with DNA. Both of them experience reduction in absorbance and red shift in λ_{max}, which is due to stabilization of the dye after binding with DNA. There is a special feature to account for, i.e. in case of these dyes their absorbances decrease on addition of DNA up to a certain concentration, after that these increase slightly with DNA. This is probably due to the formation of a loose complex between DNA and the individual individual dye. However, acridine yellow behaves in a totally different manner with DNA as its absorbance starts increasing just after the first addition of DNA (12.3 μM) and the increment gradually continues with gradual addition of DNA. The λ_{max} of acridine yellow also gets red-shifted on addition of DNA. Both these findings evidently point out the possibility of the formation of a complex in ground state between acridine yellow and DNA. Moreover, the bathochromic shift (445 nm→459 nm) carries the information in support the stabilization of the complex

Fluorescence studies:

Figure 3 (a), (b), (c) and (d) are the representative fluorescence spectra of acridine, acridine yellow, proflavine and acridine orange.

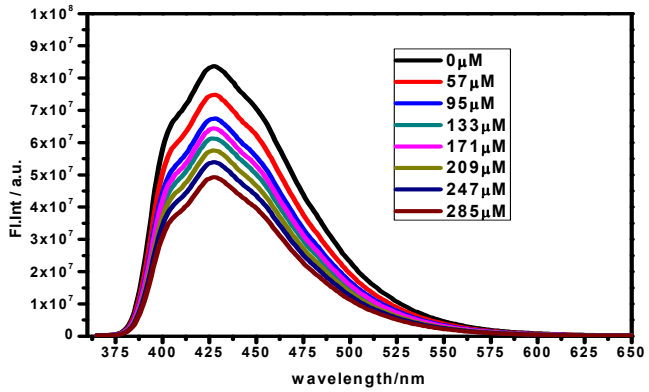

Figure 3(a): Fluorescence spectra of acridine (0.01mM) in absence and presence of varying concentration of CT DNA. (λ_{ex} =343 nm)

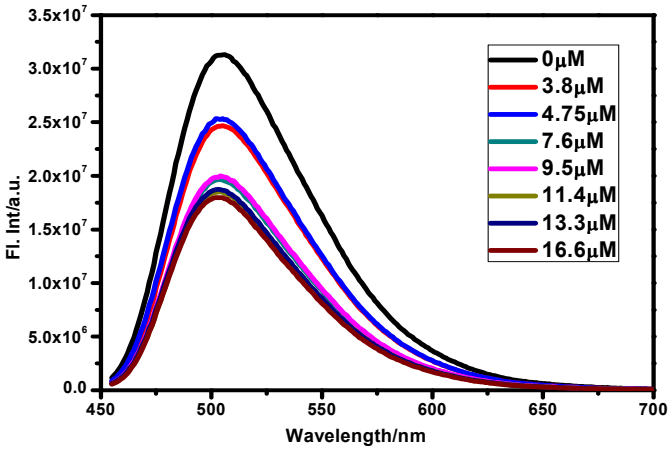

Figure 3(b): Absorption spectra of acridine yellow (0.01mM) in absence and presence of varying concentration of CT DNA. (λ_{ex} =445 nm)

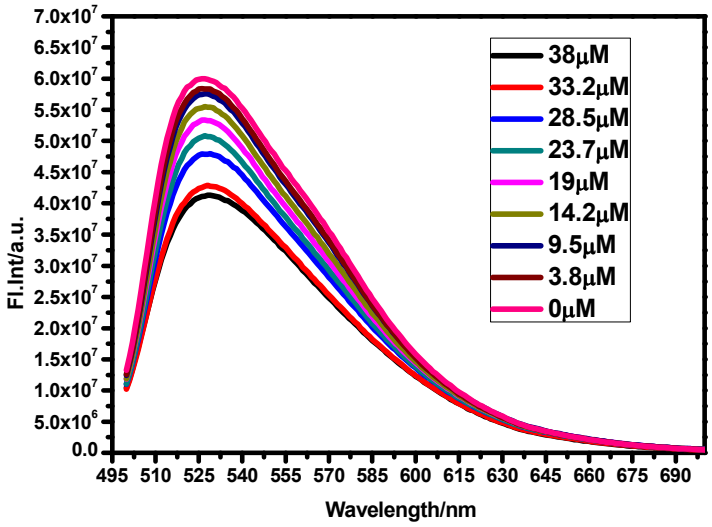

Figure 3(c): Fluorescence spectra of acridine orange (0.01mM) in absence and presence of varying concentration of CT DNA. (λ_{ex} =450 nm)

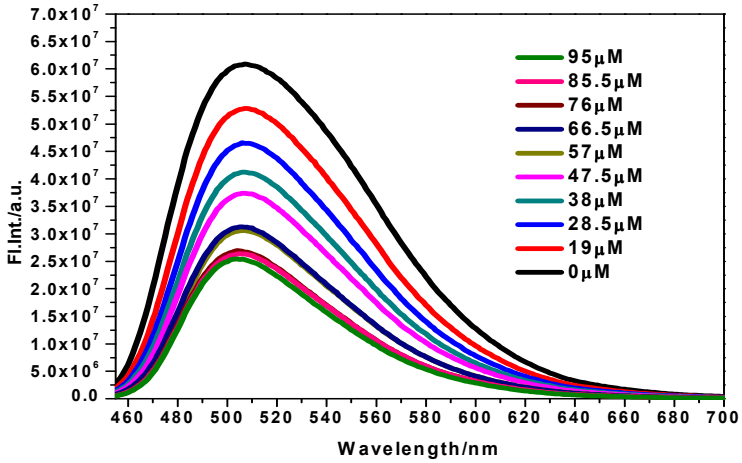

Figure 3(d): Fluorescence spectra of proflavine (0.01mM) in absence and presence of varying concentration of CT DNA. (λ_{ex} =445 nm)

The different responses in fluorescence spectra further bear striking evidences for differential behavior of these dyes in presence of DNA depending on their structure. The dissimilarity among is actually the outcome of different ground and excited state interactions of those chromophores with DNA. Steady-state fluorescence spectrum of acridine shows a quenching of fluorescence intensity upon addition of DNA without experiencing any shift in the fluorescence maximum. Acridine yellow and proflavine also undergo fluorescence quenching along with a very slight shift in fluorescence maxima (504 nm→502 nm and 506 nm→503 nm respectively).To a sharp contrast to all of them, Acridine orange experiences a gradual increase in fluorescence intensity upon addition of steadily increasing concentration of CT DNA, but hardly undergoes any change in fluorescence maximum.

The disparity in the behavior of these acridine dyes in presence of DNA is generated by the different substituents with acridine moiety. The decrement in fluorescence intensity in case of

acridine, acridine yellow and proflavin can be attributed to their participation in CT reaction with the nearby DNA bases of the intercalation site, while the presence of two $N(CH_3)_2$ groups (exerting +I and +R effect) in acridine orange makes the central acridine moiety highly electron rich to accept electrons from the neighbouring DNA bases much more compared to the others. Therefore, it shows only gradual increase in fluorescence indicating the lesser polarity and restricted solvent environment which are responsible for the annihilation of the nonradiative decay channels at the intercalation site.

The Stern volmer quenching constants (K_{SV}) have been calculated from steady-state fluorescence measurements of the dyes in absence and presence of DNA with varied concentrations following Stern-volmer equation:

$F_0/F = 1+ K_{SV}[Q] = 1+ kq.\tau_0$, where F_0 and F are the fluorescence intensities in the absence

and presence of DNA. K_{SV} is the Stern-Volmer quenching constant, k_q is the bimolecular quenching constant, which is the measure of interaction between the fluorophore and the quencher and τ_0 is the lifetime of the fluorophore in absence of any quencher.

The table below contains the values of the K_{SV} and bimolecular quenching constants (K_q) which indicate the mode of interactions of these dyes with CT DNA. A F_0/F vs. conc. of DNA plot produces the K_{sv} values.

.

Table 1: Stern Volmer Quenching Constant **(**Ksv) and Bimolecular Quenching Constant (Kq) for four different systems. τ_0 = Lifetime of the dye In absence of DNA.

System	K_{sv}/M^{-1}	τ_0/ns	$k_q/M^{-1}S^{-1}$
Acridine-DNA	$0.00236X10^6$	8.49	$1.62X10^{11}$
Acridine Yellow-DNA	$0.0522X10^6$	4.85	$1.07X10^{13}$
Proflavine-DNA	$0.00835X10^6$	4.85	$1.72X10^{12}$
Acridine Orange-DNA	$0.02317X10^6$	1.71	$1.35X10^{13}$

Time resolved fluorescence studies: The origin of the observed variation in fluorescence quenching behavior of these dyes can be confirmed from time-resolved fluorescence experiments at different time resolutions. Primarily, we have employed nanosecond-resolved TCSPC technique for time-resolved fluorescence studies. The parent derivative of acridine does not show any alteration in its excited state lifetime (8.49 ns in aqueous buffer) upon addition of DNA upto 806 μM concentration, however, the other derivatives experience the changes in fluorescence lifetime in presence of DNA quite differently

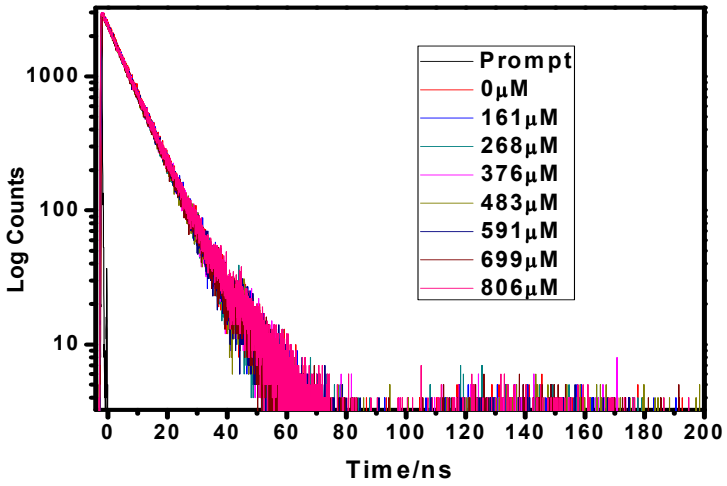

Figure:- 4(a) Fluorescence decay profile of acridine (0.01mM) in absence and presence of varying concentration of CT DNA. (λ_{ex}=377 nm, λ_{em} =427 nm)

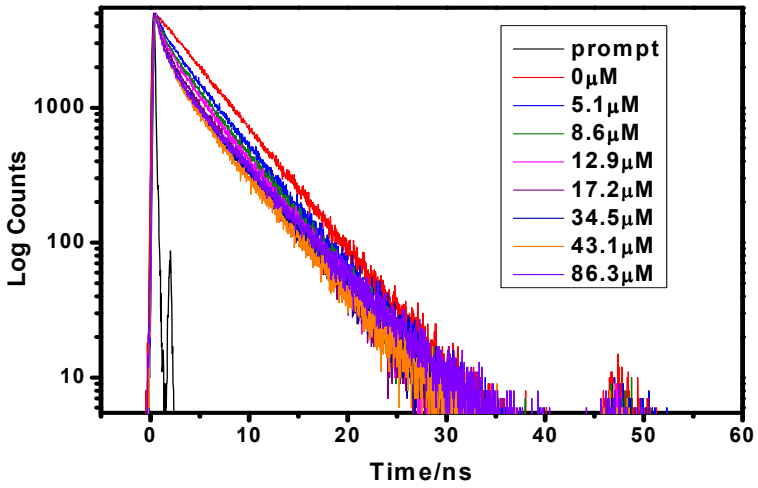

Figure:- 4(b) Fluorescence decay profile of acridine yellow(0.01mM) in absence and presence of varying concentration of CT DNA. (λ_{ex}=471 nm, λ_{em} =504 nm)

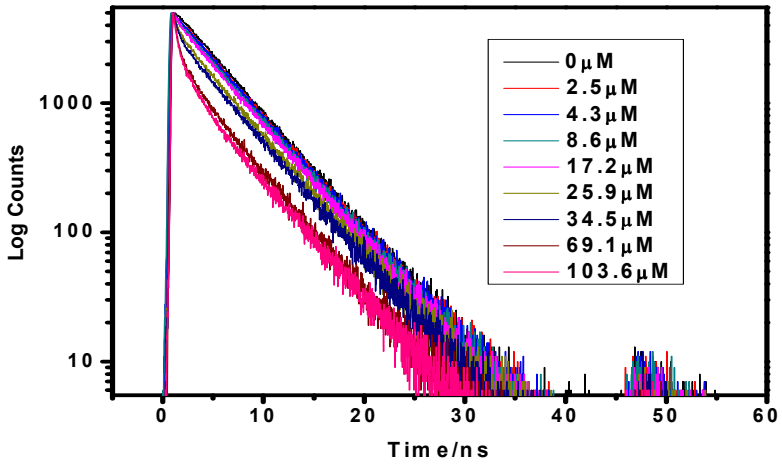

Figure:- 4(c) Fluorescence decay profile of proflavine (0.01mM) in absence and presence of varying concentration of CT DNA. (λ_{ex}=471 nm, λ_{em} =507 nm)

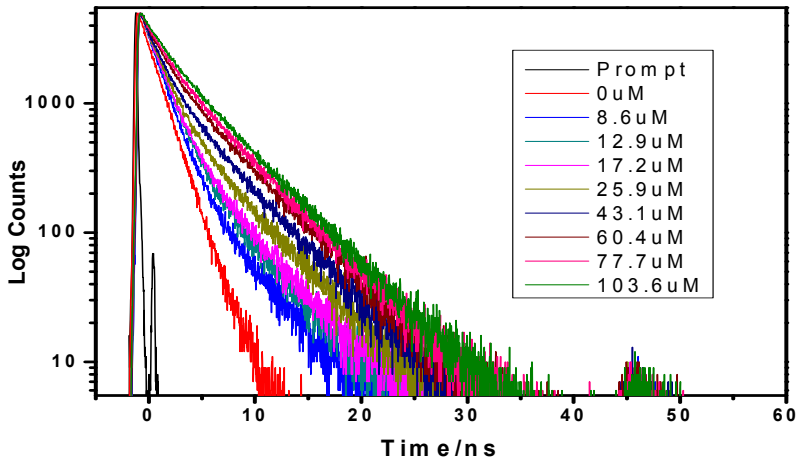

Figure:- 4(d) Fluorescence decay profile of proflavine (0.01mM) in absence and presence of varying concentration of CT DNA. (λ_{ex}=471 nm, λ_{em} =532 nm)

The tables 2, 3 & 4 show the changes in fluorescence lifetimes of proflavine, acridine yellow and acridine orange respectively with increasing concentration of DNA. In this respect acridine

yellow and proflavine behave similarly. In both the cases, the monoexponential nature of the fluorescence decay profiles changes towards biexponential while intercalated to DNA. The longer component of both the dyes (4.85 ns) does not change very much. However, a shorter time component of about ~1.3 ns and ~0.72 ns arises in case of acridine yellow and proflavine respectively after the initial addition of DNA (5.1 μM and 2.5 μM respectively). This component gets reduced upon gradual addition of DNA to some extent. The contribution of the longer time constant gradually decreases, and that of the shorter time constant increases. This observation along with the steady state fluorescence quenching of these two dyes may bear the evidences of electron transfer with DNA helix. The shorter component arising here may be the result of the electron transfer within the encounter complex formed with acridine yellow or proflavine and DNA.

On the contrary acridine orange shows the exactly opposite response in time-resolved fluorescence experiments in absence and presence of DNA. Its monoexponential fluorescence decay profile having time constant 1.71 ns in aqueous buffer changes to biexponential decay after the initial addition of 8.6 μM of DNA. A second longer component of ~ 5.07 ns arises with 16.79% contribution. Both the shorter and the longer life time increase a little bit, but their fractional contributions alter dramatically on addition of DNA. The contribution of shorter time component changes from 100% to 24.15% and the contribution of longer component changes from 16.79% to 75.85%. According to Luzzati et al.,it was proposed that acridine and its related compounds bind to DNA by intercalation between normally neighboring base pairs in a plane perpendicular to the helix axis.[20] The shorter lifetime arises probably due to the presence of some unbound drugs. The increase in shorter lifetime, although it is small, with higher DNA concentration may be due to the presence of ordered solvent environment in the vicinity of DNA

helix. The longer lifetime is due to the intercalated form of acridine orange which increases both its magnitude and percentage contributions along with increase in DNA concentration.

Till now, our results show a consistent response in lifetime changes in case of the derivatives of acridine, however, the parent molecule itself keeps it lifetime unaltered with addition of DNA.Therefore, we like to attribute its steady state fluorescence quenching not due to electron transfer, but to the overall reduction of the absorbance of the fully intercalated acridine in presence of DNA.

The percentage of the shorter lifetime components within the picosecond time regime is small in case of acridine yellow and proflavine, which deserves further investigations using femtosecond time resolution.

Table 2: Nanosecond resolved fluorescence lifetimes of Proflavine with increasing concentration of DNA (λ_{ex} =445 nm, λ_{em} = 504 nm)

DNA (μM)	τ_1(ns)/a_1 (%)	τ_2(ns)/a_2 (%)	X^2
0	4.85/100		1.39
5.1	1.29/7.56	4.79/92.44	1.53
8.6	1.21/10.46	4.75/89.54	1.47
12.9	1.12/12.53	4.71/87.47	1.32
17.2	1.18/17.48	4.74/82.52	1.39
34.5	1.23/23/02	5.07/76.98	1.25

43.1	1.15/24.88	4.97/75.12	1.19
86.3	1.15/21.74	5.38/78.26	1.2

τ_1 , τ_2 = Nanosecond life time component of dyes, a_1 , a_2 = Percentage contribution of each lifetime. X^2 = goodness of fit. (For table 2, 3, 4)

Table 3: Nanosecond resolved fluorescence lifetimes of Acridine yellow respectively with increasing concentration of DNA (λ_{ex} =445 nm, λ_{em} = 507 nm)

DNA (μM)	τ_1(ns)/a_1 (%)	τ_2(ns)/a_2 (%)	X^2
0	4.85/100		1.09
2.5	4.84/100		1.28
17.2	4.80/97.83	0.72/2.17	1.17
25.9	4.77/95.47	0.55/4.63	1.22
34.5	4.74/92.86	0.55/7.14	1.29
69.1	4.53/82.65	0.55/17.53	1.38
103.6	4.53/78.12	0.55/21.88	1.4

Table 4: Nanosecond resolved fluorescence lifetimes of Acridine orange respectively with increasing concentration of DNA (λ_{ex} =492 nm, λ_{em} = 532 nm)

DNA (μM)	τ_1(ns)/a_1 (%)	τ_2(ns)/a_2 (%)	X^2
0	1.71/100		1.5
8.6	1.69/83.21	5.07/16.79	1.42
12.9	1.81/77.12	5.26/22.18	1.51
17.2	1.79/72.16	5.22/27.84	1.43
25.9	1.83/59.70	5.27/40.30	1.35
43.1	1.83/43.99	5.19/56.01	1.40
60.4	1.93/32.49	5.21/67.45	1.31
77.7	2.05/27.26	5.25/72.74	1.29
103.6	2.29/24.15	5.33/75.85	1.17

Fluorescence upconversion studies:-

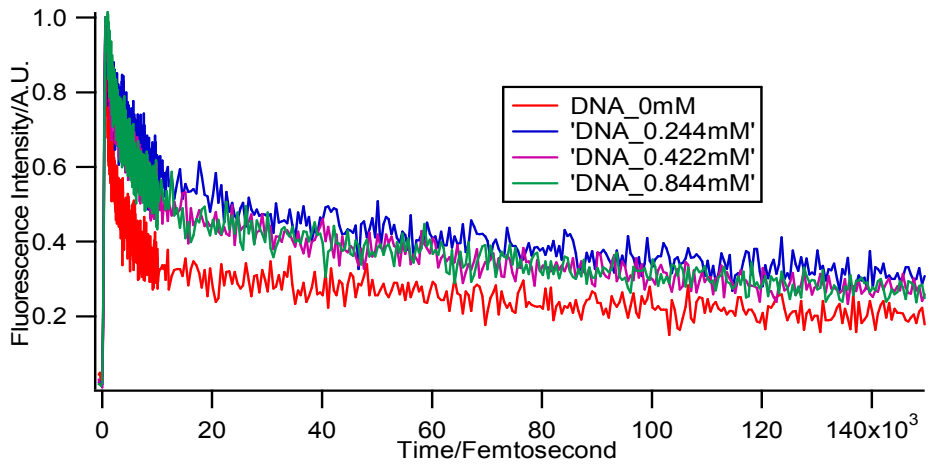

Figure:- 5(a)Femtosecond resolved fluorescence decay of transients of Acridine yellow (0.25mM) in absence and presence of varying concentration of CT DNA. (λ_{ex} =400 nm, λ_{em} = 504 nm)

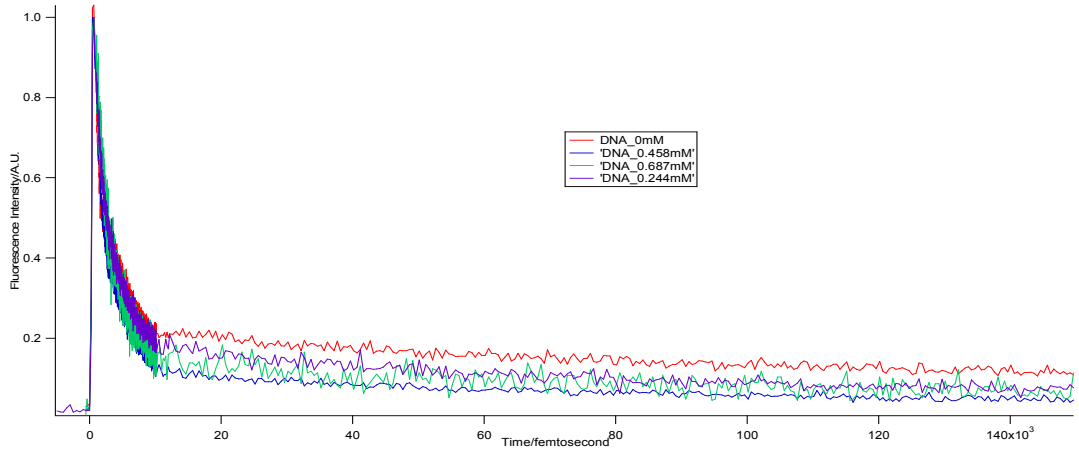

Figure:- 5(b) Femtosecond resolved fluorescence decay of transients of Proflavine (0.25mM) in absence and presence of varying concentration of CT DNA. (λ_{ex} =400 nm, λ_{em} = 507 nm)

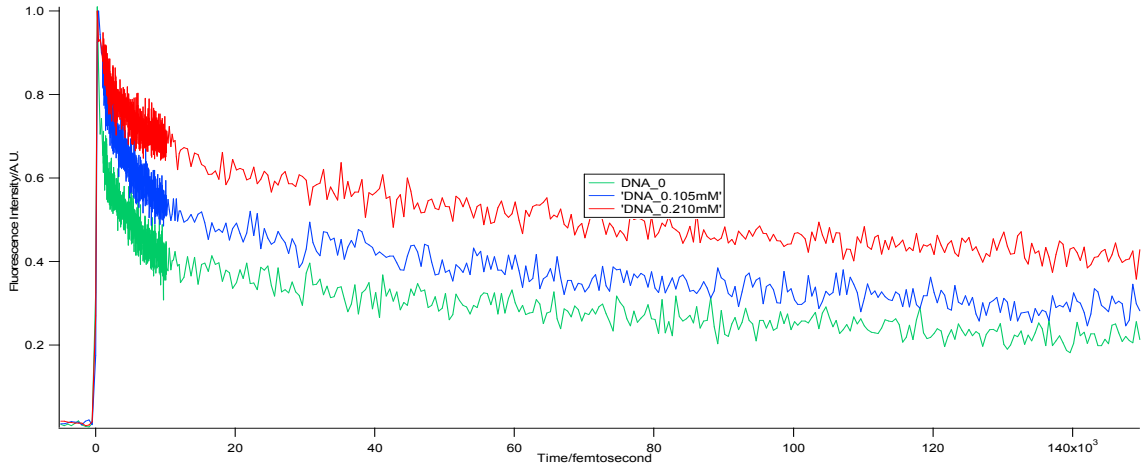

Figure:- 5(c) Femtosecond resolved fluorescence decay of transients of Acridine orange (0.25mM) in absence and presence of varying concentration of CT DNA (λ_{ex} =400 nm, λ_{em} = 530 nm).

The above figures clearly depict a change in the first component of these dyes within femtosecond-picosecond time range. Their responses with addition of CT DNA are quite different from each other. The very fast femtosecond-picosecond component reduces in case of proflavine, where this same increases in case of acridine yellow and acridine orange.

Table 5: Femtosecond resolved fluorecscence decay constants of Acridine yellow in absence and presence of varying concentration of CT DNA. (λ_{ex} =400 nm, λ_{em} = 504 nm)

[DNA]/mM	$\tau_1(a_1)$ /fs	$\tau_2(a_2)$/fs	$\tau_3(a_3)$/fs
0	285 (0.53)	3949(0.26)	263977(0.19)
0.244	351 (0.26)	6369(0.29)	219229(0.44)
0.488	430 (0.29)	5506(0.34)	217289(0.36)
0.976	826 (0.20)	5158(0.38)	202941(0.41)

Table 6 : Femtosecond resolved fluorecscence decay constants of Proflavine in absence and presence of varying concentration of CT DNA. (λ_{ex} =400 nm, λ_{em} = 507 nm)

[DNA]/mM	$\tau_1(a_1)$/fs	$\tau_2(a_2)$/fs	$\tau_3(a_3)$/fs
0	267(0.51)	5416(0.22)	227562(0.27
0.105	999(0.22)	9967(0.18)	282281(0.59)
0.210	1128(0.22)	13204(0.20)	360828(0.57)

Table 7 : Femtosecond resolved fluorecscence decay constants of acridine orange in absence and presence of varying concentration of CT DNA. (λ_{ex} =400 nm, λ_{em} = 532 nm)

[DNA]/mM	τ_1 (a_1)/fs	τ_2 (a_2)/fs	τ_3 (a_3)/fs
0	391(0.59)	4490(0.31)	373473(0.083)
0.244	445(0.38)	5602(0.50)	488114 (0.11)
0.487	601(0.36)	7928(0.43)	632487(0.21)

τ_1, τ_2, τ_3 = femtosecond resolved life time component of dyes, a_1, a_2, a_3 = Percentage contribution of each lifetime. (For all table 5, 6, 7)

The differential trend of lifetime changes, as indicated from Table 5, 6 & 7 for acridine yellow, proflavine and acridine orange respectively, should be attributed to the structural parameters of these dyes. Proflavine, being a simple molecule (only containing $–NH_2$ group as substituent), intercalates in DNA and its lifetime gets reduced due to direct electron transfer (in femtosecond, picosecond and nanosecond timescale) from the neighboring bases. Acridine yellow undergoes a reduction in lifetime in nanosecond time range; however in femtosecond-picosecond time range its lifetime increases. Acridine yellow has flanking $–NH_2$ and $-CH_3$ group, therefore, it takes a little more time to intercalate properly inside DNA environment and to have proper orientation for occurrence of electron transfer from the bases which are reflected in the decrease of nanosecond lifetime due to electron transfer and in the increase of picosecond lifetime that is due to its constrained solvation at DNA intercalation site.

Acridine orange, as it contains -$N(CH_3)_2$, the central moiety gets too much electron rich to accept electron. Therefore, even in faster timescale the time constants increase owing to slower solvation in DNA environment. Dynamics of water exchange with bulk has already shown to play a vital role in controlling the solvation free energy of drug−DNA interactions.[34] Earlier Zewail and his co-workers detected two time components of 1 ps and 10-12 ps in the temporal time resolution of femtosecond for DNA hydration by two different types of water molecules. The slower hydration is for 'dynamically ordered water' which plays an important role in molecular recognition.[21] In our case, addition of DNA into these dyes may introduce this kind of ordered water environment, where acridine orange gets solvated and its fluorescence decay slows down by means of slower relaxation of its radiative channels, which is reflected in the longer decay times (Table 7). This finding could be even supported by other literatures also. Banerjee et al. showed that another dye molecule DAPI, although it is a minor groove binder, shows similar increase in intensity while binding to random sequence CT DNA due to its residence in hydrophobic environment.[37]

Although in our case, dynamics of intercalation and subsequent ET have been tested only with random sequence calf thymus DNA, several other groups affirmed the role of solvation of a dye molecule by the 'ordered water environment' by changing the base sequence, which evidently notifies that local structure of DNA helix can alter the rigidity of solvent molecular framework that reflects in time scale of subpicosecond fluorescence lifetime of a dye. Verma et al. reported that the local hydration of DAPI is dependent even on a single base variation near the ligand binding site.[38]

Time-resolved anisotropy

Anisotropy in fluorescence measurement in solution arises due to several reasons. While steady state anisotropy gives the measure of micro-environmental inhomogeneity around the probe location, the time-resolved anisotropy depicts the constraints on the rotational correlation time $<\tau_r>$ of the probe in solution.[22,23-28] Here, we try to have an idea on the extent of microheterogeneity near the intercalation sites of CT DNA by means of rotational time constants of those dyes. (Table 8)

Table 8 below depicts the rotational time constants in buffer and in presence of CT DNA (concentration of CT DNA was kept as for highest anisotropy)

System	τ_{buff}	τ_{1DNA}	τ_{2DNA}	θ_w/Deg
Acridine Yellow-DNA	213ps	324ps(4.36%)	8.26ns(95.64%)	61.92 deg
Proflavine-DNA	212 ps	338ps(18.25%)	5.79ns(81.75%)	64.26deg
Acridine Orange-DNA	209 ps	291ps(9.90%)	6.29ns(90.10%)	62.30deg

The above mentioned time constants undoubtedly affirm the presence of motional restriction at the DNA intercalation site. The DNA unbound drug always shows a single exponential decay, while addition of a higher concentration of CT DNA makes the rotational relaxation profile

biexponential. This biexponential decay profile may be attributed to the two forms of the dyes, one is intercalated and the other is bound to the surface of DNA, which are responsible for the longer and the shorter time components respectively.

This biexponential decay behavior of these acridine derivatives can also be interpreted in terms of two-step and wobbling-in-cone model. The functional form of the biexponential anisotropy decay, r(t), can be represented as,

$r(t) = r(0) \times [a_{1r} \exp(-t/\tau_{1r}) + a_{2r} \exp(-t/\tau_{2r})]$, [22]

where r(0) is the limiting anisotropy or the inherent fluorescence depolarization of the probe, a_{ir} is the preexponential factor of the i^{th} component of the relaxation time (τ_{ir}). The generalized order parameter S, which is actually a measure of degree of restriction on the wobbling in cone orientational motion, is depicted as, $S^2 = a_{2r}$.Itranges from 0 to 1.The value of the semicone angle (θ_w) has been calculated from the value of order parameter (S), by the equation follows:

$S=1/2\ \cos\theta_w(1+\cos\theta_w)$, The values of θ_w are calculated for three Drug-DNA systems and tabulated in the above table.[22, 23-28]

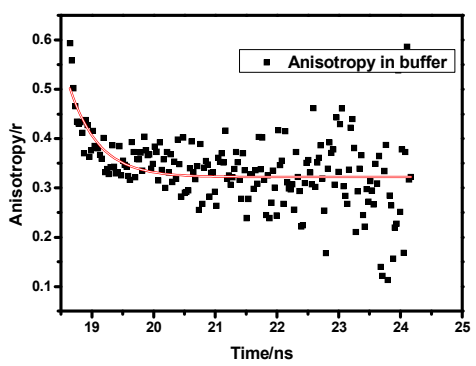

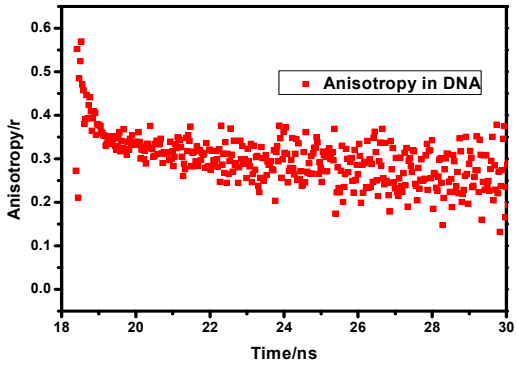

Figure:-6. Time resolved fluorescence anisotropy decay transients of Acridine yellow (0.01mM) in (a) absence and (b) presence of CT DNA

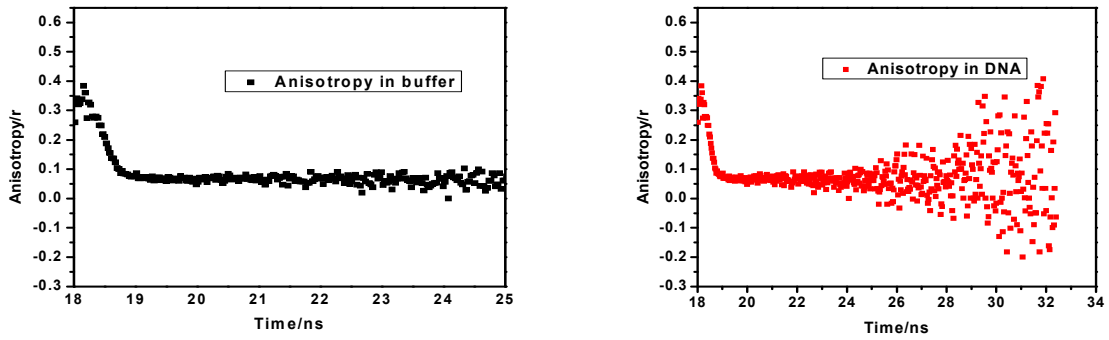

Figure:-7. Time resolved fluorescence anisotropy decay transients of Acridine orange (0.01mM) in (a) absence and (b) presence of CT DNA

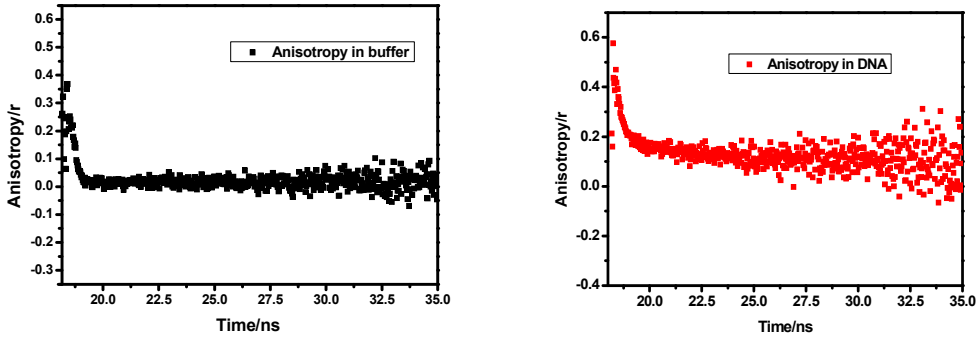

Figure:-8. Time resolved fluorescence anisotropy decay transients of Proflavine (0.01mM) in (a) absence and (b) presence of CT DNA.

Circular Dichroism Studies:-

Intercalation of small molecules may lead to the changes in the conformation of the double helical DNA strand. It can cause stabilization as well as destabilization to DNA. [29, 30] The perturbation in the secondary structure of DNA upon interaction with the drug molecule has been studied by circular dichroism. The far-UV CD spectra (220–320 nm) of DNA in aqueous buffer exhibits a typical shape, revealing a minimum at ~247 nm and a maximum at ~276 nm corresponding to the right handed B-form. On the addition of these aforementioned drugs the CD profile undergoes a considerable change at both its positive and negative peak positions at ~247 nm and ~276 nm. [31] It is said that the groove binding and ionic interaction lead to only a minor perturbation in DNA backbone structure, hence in circular dichroic spectral profile. However here, the enhancement of the band at ~276 nm can be attributed to the disruption of the stacking interaction between the base pairs for intercalation of the dye molecule.[32] Thus, the signatures in the CD profiles confirm the binding mode of all these four dyes to be intercalative with DNA.

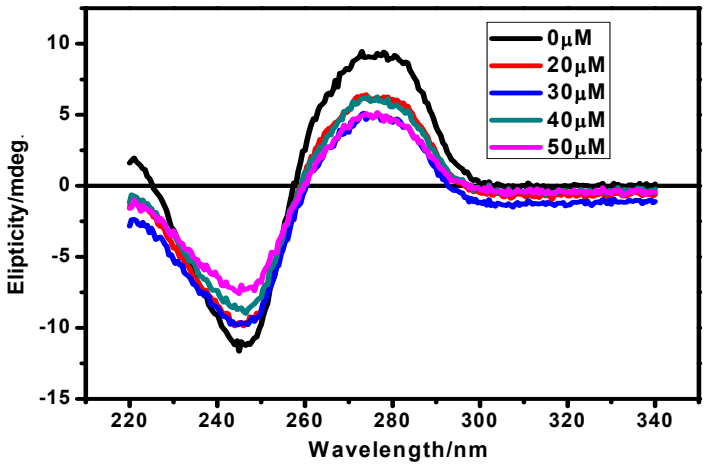

Figure 9(a): Circular dichroic spectral profile of DNA (50 mM) with increasing Acridine yellow concentration. Y axis is plotted as Elipticity/mill degree.

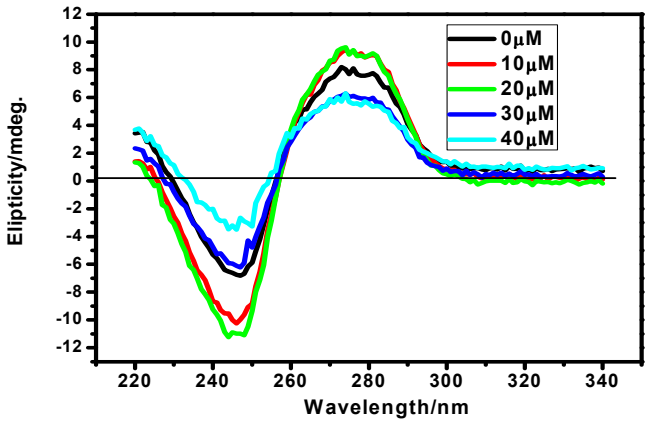

Figure 9(b): Circular dichroic spectral profile of DNA (50 mM) with increasing Acridine concentration

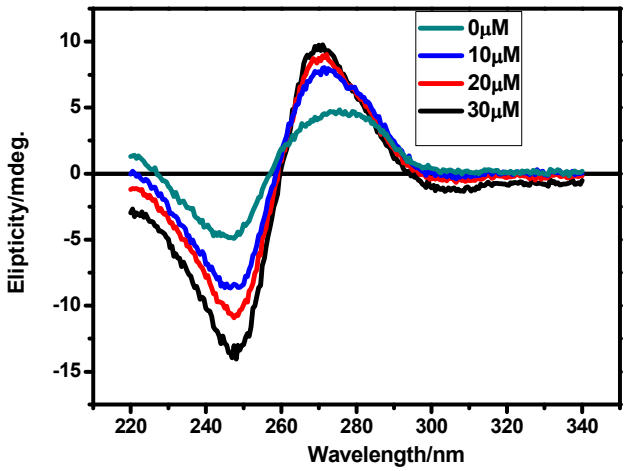

Figure 9(c): Circular dichroic spectral profile of DNA (50 mM) with increasing Proflavine concentration

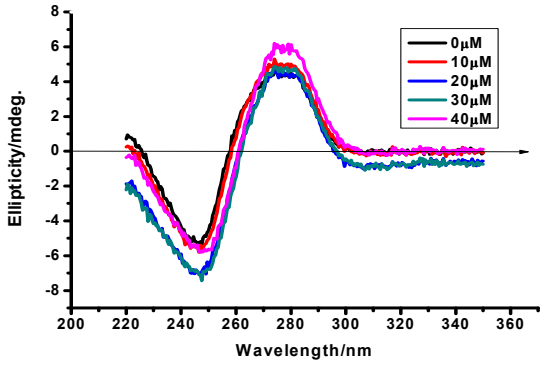

Figure 9(d): Circular dichroic spectral profile of DNA (50 mM) with increasing Acridine orange concentration.

Viscometric Analysis:

The viscometric analysis also supports the trend of intercalation of these four drugs into DNA. Usually, Intercalation of small molecules into DNA leads to increasing in viscosity by means of lengthening of DNA. In our case, full intercalation of acridine causes the highest change in viscosity followed by proflavine, acridine yellow and acridine orange. Owing to largest substituents, acridine orange probably gets only partial intercalation causing a very small change in DNA length. The figures below depict clearly the trend in the relative viscosity change (η/η_0) with change in the concentration of added.

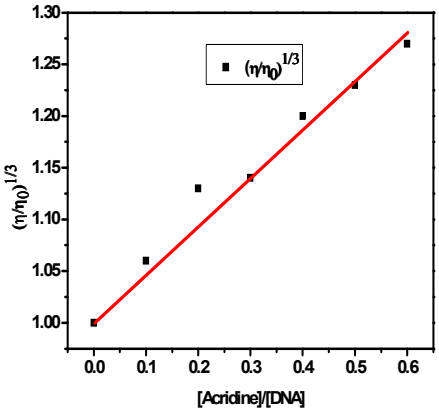

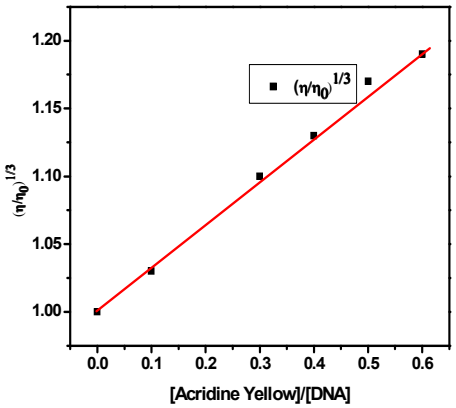

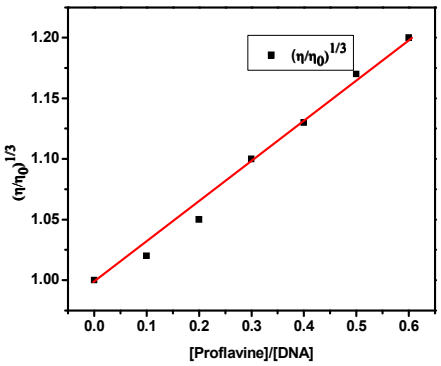

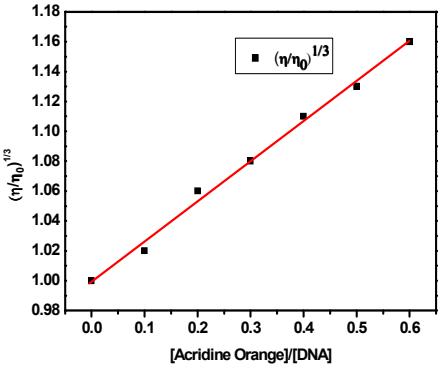

Figure 10: Relative viscosity of CT-DNA (103 μM) with varying concentration of Acridine, Acridine Yellow, Proflavine and Acridine Orange respectively at pH 7.4 at room temperature.

Conclusion

It is well known that the common acridine derivatives are bound in DNA environment through intercalation. However, in the present study it has been attempted to identify some other electronic and steric factors, which can induce some specific dynamic features over intercalation, for respective dye molecule while interacting with DNA. Our studies from the series of spectroscopic investigation could infer that these drug molecules have a systematic electronic control on the consecutive steps of intercalation, solvation and PET which is rarely reported in literature. Primarily all the dyes are intercalative, but their individual mode of intercalation largely depends on the functional groups present on the central acridine moiety and that is reflected in their absorption as well as in static and dynamic fluorescence behavior. Acridine undergoes a complete intercalation inside DNA, whereas its other derivatives involve dynamic as well as partial intercalation. Moreover complexation and charge transfer behavior of these dyes with DNA are quite different from each other. We have tried to probe the individual steps of intercalation which occur in different time scale depending on their structural parameters. Previously, von Feilitzsch et al reported similar structural control of 9-Amino-6-chloro-2-methoxyacridine tethered by a -$(CH_2)_6$-Linker regarding DNA intercalation and showed that long chain flanking substituent leads to partial intercalation within the base stack and probably gets attached to the nearby phosphate groups, which in turn also affects PET, as in our case. The fluorescence dynamical behavior of the fluorescent dyes undoubtedly proves that charge transfer

from neighboring DNA bases at intercalation site is primarily dependent on the electron density of the central acridine moiety.[16] Moreover; this particular investigation on dynamics of complex water structure is further valuable for understanding the DNA-protein and drug-DNA recognitions *in vitro* and *in vivo*. Contribution of electronic and steric factors of drugs in DNA binding and subsequent ET may lead to an arena of drug designing and delivery system. Therefore, probing the fluorescence dynamics of the bound drug using different types of spectroscopy is an easy way to get information about the water dynamics near DNA vicinity. Here, the ordered water environment at the proximity of DNA strand clearly depicts the extent of solvation of the individual drug which occurs within few picosecond probed by femtosecond resolved fluorescence upconversion spectroscopy.

Acknowledgment: We would like to acknowledge Banabithi Koley Seth, SINP for her suggestions during this work. Moreover, we are also thankful to Prof. Debabrata Mandal of University of Calcutta to provide us igorpro software for analysis. This work has been funded by Biomolecular Assembly, Recognition and Dynamics (BARD) projects, Saha Institute of Nuclear Physics of Department of Atomic Energy (DAE), Government of India.

References:-

1. D.D. Eley, D.I. Spivey, *Trans. Faraday Soc.*1962, **58**, 411

2. J.K. Barton, C.V. Kumar, N.J. Turro, *J. Am. Chem. Soc.*1986, 108, 6391.

3. P. O'.Neill, E.M. Frieden, In Advances in Radiation Biology: DNA and Chromatin Damage Caused by Radiation.*ed. J. T. Lett and W. K. Sinclair, Academic Press, New York* 1993, **17**, 53.

4. B. Armitage, *Chem. Rev.***1998**, *98*, 1171–1200.

5. C.J. Burrows, J.G. Muller, *Chem. Rev.*1998, **98**, 1109.

6. D. Wang, D.A. Kreutzer J.M. Essigmann, *Mutat. Res.Fundam. Mol. Mech. Mutagen.*1998, **400**, 99.

7. S. Kawanashi, Y. Hiraku, S. Oikawa, *Mutat.Res., Rev. Mutat. Res.*2001, **488**, 65.

8. J. Merino, A.K. Boal, J.K. Barton, *Curr. Opin. Chem. Biol.***2008**, *12*, 229.

9. F.Boussicault, M. Robert, *Chem. Rev.*2008, **108**, 2622.

10. M.A. O'Neill, J.K. Barton, *J. Am.Chem. Soc.*2004, **126**, 13234.

11. J.C. Genereux, K.E. Augustyn, M.L. Davis, F, Shao, J.K. Barton, *J. Am. Chem. Soc.*2008, **130**,15150.

12. L. Brillouin, Horizons in Biochemistry. Kasha, M.; Pullman, B.; editors. New York City: Academic Press; 1962, 2951962.

13. V.V. Zakjevskii, S.J.King, O. Dolgounitchevam, V.G. Zakrzewski, J.V. Ortiz, *J. Am. Chem. Soc.*2006, **128**, 13350.

14. D.M. Close, K.T. Øhman, *J. Phys. Chem. A* 2008, **112**, 11207.

15. V. Gabelica, F. Rosu, T. Tabarin, C. Kinet, A. Rodolphe, M. Broyer, E. De Pauw, P. Dugourd, *J. Am. Chem. Soc.,* 2007, **129**, 4706-4713.

16. W.B. Davis, S. Hess, I. Naydenova, R. Haselsberger, A. Ogrodnik, M.D. Newton, M.E. Michel-Beyerle, *J. Am. Chem. Soc.,* 2002, **124**, 2422.

17. T. von Feilitszch, J. Tuma, H. Neubauer, L. Verdier, R. Haselsberger R. Feick, G. Gurzadyan, A.A. Voityuk, C. Griesinger, M.E. Michel-Beyerle, *J. Phys. Chem B,* 2008, **112**, 973-989.

18. S. Hess, W.B. Davis, A.A.Voityuk, N. Rosch, M.E. Michel-Beyerle, N.P. Ernsting, S.A. Kovalenko, J.L. Perez Lustres, *ChemPhysChem*, 2002, **5**, 452.

19. E. Kuruvilla, D. Ramaiah, *J. Phys. Chem. B* 2007, **111**, 6549 .

20. V. Luzzati, F. Masson, L.S. Lerman, *J Mol Biol.* 1961, **3**, 634.

21. S.K. Pal, J. Peon , B. Bagchi , A.H. Zewail, *J. Phys. Chem. B*, 2002, **106 (48)**, 12376.

22. Lakowicz, J. R. Principles of Fluorescence Spectroscopy; Plenum: New York, 1999.

23. K. Kinosita, S. Kawato, A. Ikegami, *Biophys. J.* 1977, **20**, 289.

24. G.B. Dutt, *J. Phys. Chem. B* 2005, **109**, 4923.

25. E.L. Quitevis, A.H. Marcus, M.D, Fayer, *J. Chem. Phys.* 1993, **97**, 5792.

26. A. Chakraborty, D. Seth, P. Setua, N. Sarkar, *J. Chem. Phys.* 2008, **128**, 204510.

27. C.E. McKenna, B.A. Kashemirov, T.G.Upton, V.K. Batra, M.F. Goodman, L.C. Pedersen, W.A. Beard, S.H. Wilson, *J. Am.Chem. Soc.* 2007, **129**, 15412.

28. D. Sahoo, P. Bhattacharya, S. Chakravorti, *J. Phys. Chem. B* 2010, **114**, 2044.

29. S.S. Jain, A. Matjaz, N.V. Hud, *Nucleic Acids Res.* 2003, **31**, 4608.

30. J.L.Mergny, G. Duval-Valentin, C.H. Nguyen, L. Perrouault, B. Faucon, M. Rougee, T. MontenayGarestier, E. Bisagni, C. Helene, *Science* 1992, **256**, 1681.

31. Y.F. Long, Q.G. Liao, C. ZhiHuang, J. Ling, Y.F.Li, *J. Phys.Chem. B* 2008, **112**, 1783.

32. D. Sarkar, P. Das, S. Basak, N. Chattopadhyay, *J. Phys. Chem.B* 2008, **112**, 9243.

33. A. Ganguly, B. K. Paul, S. Ghosh, S. Dalapati , N. Guchhait, *Phys. Chem. Chem. Phys*.,2014, **16**, 8465.

34. Mukherjee, A.; Lavery, R.; Bagchi, B.; Hynes, J. T. On the molecular mechanism of drug intercalation into DNA: a simulation study of the intercalation pathway, free energy, and DNA structural changes. *J. Am. Chem. Soc*. 2008, **130**, 9747−9755.

35. Porsch, B.; Laga, R.; Horsky,J.; Konak,C.; Ulbrich, K. Molecular Weight and Polydispersity of Calf-Thymus DNA: Static Light-Scattering and Size-Exclusion Chromatography with Dual Detection. *Biomacromolecules* 2009, **10**, 3148–3150.

36. Banerjee, D.; Pal, S.K. Dynamics in the DNA Recognition by DAPI: Exploration of the Various Binding Modes, *J. Phys. Chem B* 2008, **112 (3)**, 1016–1021.

37. Verma, S.D.; Pal, N.; Singh, M.K.; Sen, S. Sequence-Dependent Solvation Dynamics of Minor-Groove Bound Ligand Inside Duplex-DNA, *J. Phys. Chem B,* ASAP.

38. Alexander, P.; Block, R. J.; Determination of the Size and Shape of Protein Molecules: A Laboratory Manual of Analytical Methods of Protein Chemistry (Including Polypeptides), Volume 3", *Elsevier,* 2014*,* **Chapter 5**.

Table of Contents:-